

Delayed Rebounds in the Two-Ball Bounce Problem

Sean P. Bartz*

*Dept. of Chemistry and Physics, Indiana State University
Terre Haute, IN 47809*

July 31, 2020

Abstract

In the classroom demonstration of the two-ball drop, some conditions lead to a “delayed rebound effect,” with the second bounce of the upper ball higher than the first. This paper uses two models to explore the causes of this phenomenon. The classic independent contact model (ICM) is reviewed for the first bounce, and extended semi-analytically to the second bounce in the perfectly elastic case. A dynamical model based on a linear dashpot force is studied numerically. The delayed rebound effect is found for a range of parameters, most commonly in cases where the first bounce is lower than the ICM prediction.

1 Introduction

In a classic classroom demonstration of linear momentum conservation, a tennis ball is held above a basketball, and the two are simultaneously dropped to the floor. Surprisingly, the tennis ball rebounds much higher than the drop height. Textbook explanations suggest that when the upper ball is much less massive than the lower ball, it rebounds at three times the impact speed, bouncing to nine times the initial drop height [1, 2, 3].

Taking this theoretical prediction to heart, I brought a ping-pong ball for an in-class demonstration, alerting students to expect a bounce more impressive than the tennis ball’s due to the larger mass disparity. The demo was a dud, with the ping-pong ball staying close to the basketball on the first bounce. However, with the balls carefully aligned, the small first bounce was followed by a noticeably higher second bounce. This paper will show that this “delayed rebound effect” is robust, and can be explained with a simple force model.

The classic justification for the high bounce of the tennis ball assumes that the basketball-floor collision is independent of the basketball-tennis ball collision. Closer inspection indicates that the simplifying assumption of this independent contact model (ICM) is invalid – the lower ball often remains in contact with the floor when the two balls first make contact.

*sean.bartz@indstate.edu

Interestingly, ICM predictions are fairly accurate in many cases when the collisions are not truly independent. However, when the initial separation between the two balls is small, the final velocities can differ greatly from the ICM prediction, particularly when the balls are allowed to bounce more than once.

Impact mechanics is relevant in a variety of fields including engineering, granular materials, and molecular dynamics. Study of this simple toy model may inform simulations in these practical applications by demarcating the conditions under which the ICM model is useful, and where more detailed simulations are required to accurately reflect macroscopic effects. Detailed study of two-particle interactions can also be extended to chain collisions of multiple particles in a line [4, 5, 6, 7, 8].

The organization of this paper is as follows: the independent contact model is described in section 2. Section 3 develops a dynamic description of the system using a linear dashpot model. Section 4 uses the linear dashpot force to examine the details of the collisions in the first bounce, and examines the rebound height of the upper ball for both the first and second bounce.

2 Independent Contact Model

The classic textbook solution to the two-ball drop problem assumes independent, instantaneous collisions between the balls and the floor. We review the ICM here to form a basis of comparison for the more-realistic dynamic model, and to introduce notation. We also extend the model to a second bounce for the elastic case.

Inelastic collisions are characterized by a coefficient of restitution, defined as the ratio of the relative velocity of the particles post-collision to their pre-collision relative velocity,

$$\varepsilon = \left| \frac{v'_1 - v'_2}{v_1 - v_2} \right|. \quad (1)$$

Here, primed velocities refer to the velocity just after the collision. Using this relation, along with conservation of momentum, the post-collision velocities are

$$v'_1 = \frac{v_1 + \mu(v_2 + \varepsilon(v_2 - v_1))}{1 + \mu} \quad (2)$$

$$v'_2 = \frac{\mu v_2 + v_1 + \varepsilon(v_1 - v_2)}{1 + \mu}, \quad (3)$$

where $\mu = m_2/m_1$.

For the stacked ball drop, we define z_1 as the distance between the bottom of the lower ball and the floor and z_2 as the height of the upper ball, as measured from the top of the lower ball when it rests on the floor (assuming the ball does not compress). See Figure 1 for an illustration. This coordinate definition, where $z_1 = 0$ and $z_2 = 0$ do not occur at the same physical point, explicitly removes reference to the radii of the balls, allowing us to extract universal behavior. The balls are assumed to move in the vertical direction only. The results of the ICM from [9] can be applied to our coordinate definition by taking the limit that the ball radii go to zero.

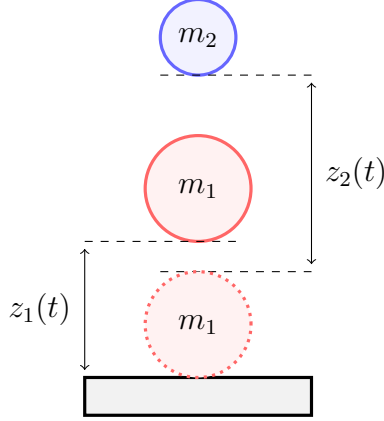


Figure 1: Coordinate definitions: z_1 is measured from the floor to the bottom of the lower ball. The coordinate for the upper ball, z_2 , is measured from the top of the lower ball when it rests on the floor without compression.

We define the drop height $h = z_1(0)$ and the gap $\Delta h = z_2(0) - z_1(0)$. Using conservation of energy, we can extend the results of [9] to calculate the maximum height of the upper ball after the first bounce

$$h_1 = \frac{h((\mu - \varepsilon(2 + \varepsilon))^2 + \Delta h(1 + \mu)(\mu - \varepsilon))}{(1 + \mu)^2}. \quad (4)$$

2.1 Delayed rebound effect in elastic ICM

Analytical description of subsequent bounces is possible, but presents practical challenges. The primary challenge is the lower ball bouncing on the floor one or several times before contacting the upper ball a second time. The trajectory of the lower ball must therefore be described in a piecewise fashion, precluding a general algebraic solution for the second collision. Because a numerical solution is necessary in any case, we do not exhaustively examine the second-bounce effect in the ICM. Rather, we examine perfectly elastic collisions with no initial gap between the balls as an illustrative example.

In this section, we take $t = 0$ to be the time of the first collision. The velocity of a perfectly elastic single bouncing ball is a sawtooth function, which can be written

$$v_1(t) = \frac{2v_1'}{\pi} \arctan\left(\cot \frac{\pi t}{t_b}\right), \quad (5)$$

where where v_1' is the post-collision velocity (2) with $\varepsilon = 1$ and $v_1 = \sqrt{2gh}$. The time scale $t_b = 2v_1'/g$ is the time a ball will spend between bounces. This model is valid only for $\mu < 1/3$, as the post-collision velocity (2) is negative for greater values, making (5) invalid.

Conservation of energy gives a direct calculation of the vertical position from the velocity

$$z_1(t) = \frac{v_1'^2}{2g} - \frac{2v_1'^2}{\pi g} \arctan^2\left(\cot \frac{\pi t}{t_b}\right). \quad (6)$$

The second collision occurs when $z_2(t_c) = z_1(t_c)$, with t_c the time of the second collision between the two balls. This reduces to the simple expression

$$v_1'^2 - v_1^2(t_c) = v_2'^2 - v_2^2(t_c). \quad (7)$$

Inserting (5) and using free-fall kinematics for the upper ball yields

$$v_2'^2 - (v_2' - gt_c)^2 = v_1'^2 - \frac{4v_1'^2}{\pi^2} \arctan^2 \left(\cot \frac{\pi t_c}{t_b} \right). \quad (8)$$

This transcendental equation is solved numerically for t_c , from which the position and velocities of the balls at their second collision are calculated. The velocities following the second collision are calculated via (2) and (3), and the height of the second bounce is calculated using free-fall kinematics.

The heights for the first and second bounce for various values of μ are shown in Figure 2, normalized by the initial drop height. In the limit $\mu \rightarrow 0$, the well known first-bounce velocity ratio of 3 is recovered, which leads to the ball bouncing to 9 times its drop height. The second bounce approaches a limit of 25.

While this simple case of the ICM shows a delayed rebound effect for a range of μ values, the quantitative predictions do not comport with informal observations. Namely, high second bounces are generally observed in situations where the first bounce is not large compared to the drop height. However, the ICM results show that the existence of the delayed rebound effect does not depend on the details of the interaction between the balls, and suggest that it is more prominent at smaller μ values, matching observations and the model results reported in the following sections.

3 Linear dashpot force

Following the work in [9] we use a linear dashpot force as a simplified approximation of the Hertz contact force between viscoelastic spheres [5, 10]. The force is

$$F_{ij} = -\min[0, -k\xi_{ij} - \gamma_j\dot{\xi}_{ij}], \quad (9)$$

where the mutual compression is defined by

$$\xi_{ij} = \Theta(-z_i + z_j), \quad (10)$$

where z_i are the vertical positions of the balls as defined in Figure 1 and $\Theta(x)$ is the Heaviside step function. The floor is denoted by index 0, while the lower and upper balls are labeled by index 1 and 2, respectively. The force definition (9) ensures that the force is always repulsive.

To simplify the analysis, the restoration constant k is taken to be the same for both balls, and the coefficient of restitution is set by varying the damping constants γ_i . The balls are considered to be in contact when the force between them is nonzero, rather than when the mutual compression is nonzero. In the case of $\gamma = 0$, the collision is perfectly elastic, and the ICM is reproduced when the initial gap Δh is large enough that the collisions are independent.

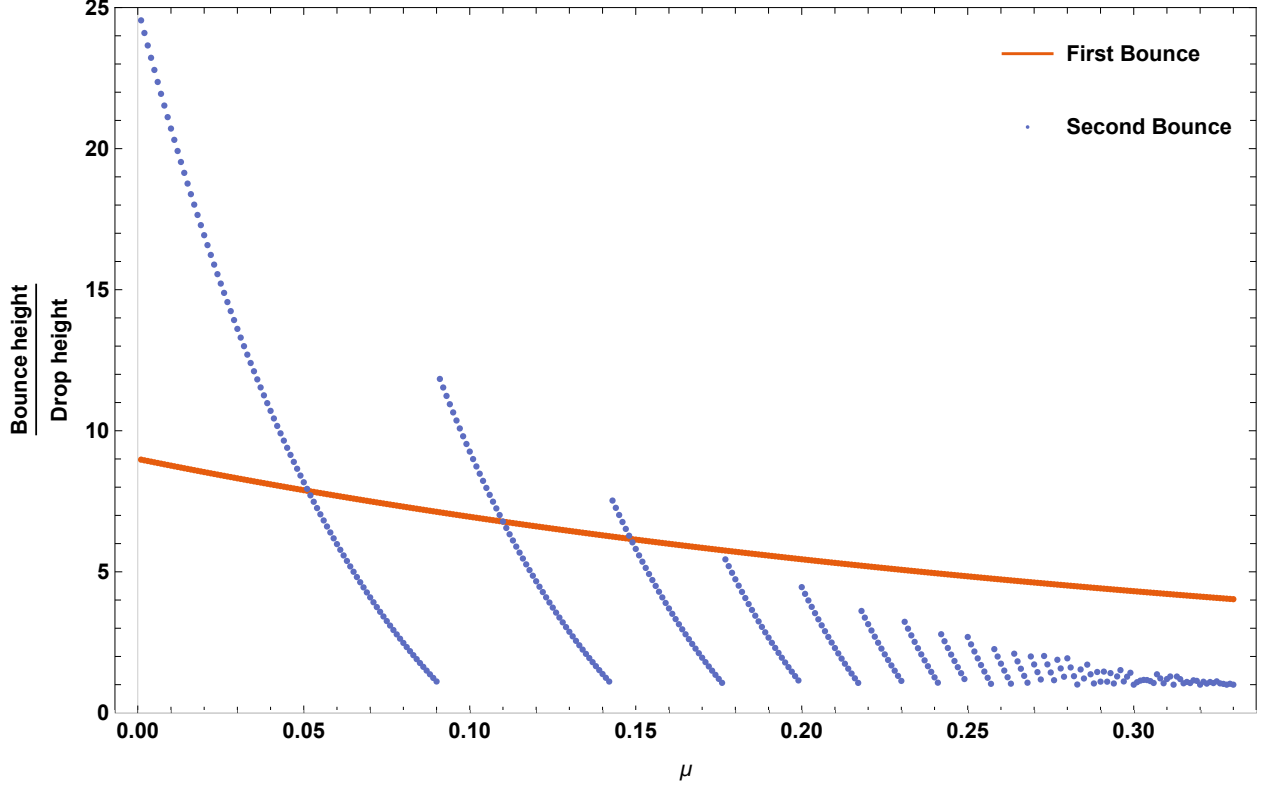


Figure 2: The bounce height of the upper ball, normalized by the initial drop height of the upper ball, shows the “delayed rebound effect” is present in the ICM for perfectly elastic collisions. In the limit $\mu \rightarrow 0$, the well-known ratio of 9 is recovered for the first bounce, and the second bounce approaches a limit of 25.

The equations of motion are

$$m_1 \ddot{z}_1 = -m_1 g + F_{01} - F_{12} \quad (11)$$

$$m_2 \ddot{z}_2 = -m_2 g + F_{12} \quad (12)$$

To isolate the parameters of physical importance, the equations of motion are written in a dimensionless fashion. The equations are non-dimensionalized via the substitutions $z_i = x_c X_i$ and $t = t_c \tau$, where $x_c = m_1 g / k$ and $t_c = \sqrt{m_1 / k}$. The equations become

$$X_1'' = -1 + f_{01} - f_{12} \quad (13)$$

$$X_2'' = -1 + f_{12} / \mu, \quad (14)$$

where (\prime) indicates a derivative with respect to τ . The dimensionless forces are

$$f_{ij} = -\min [0, \Xi_{ij} + 2\zeta_j \Xi'_{ij}] \quad (15)$$

where $\zeta_i = \gamma_i / 2\sqrt{m_1 k}$ are the damping ratios and $\Xi_{ij} = \Theta(-X_i + X_j)$ is the dimensionless

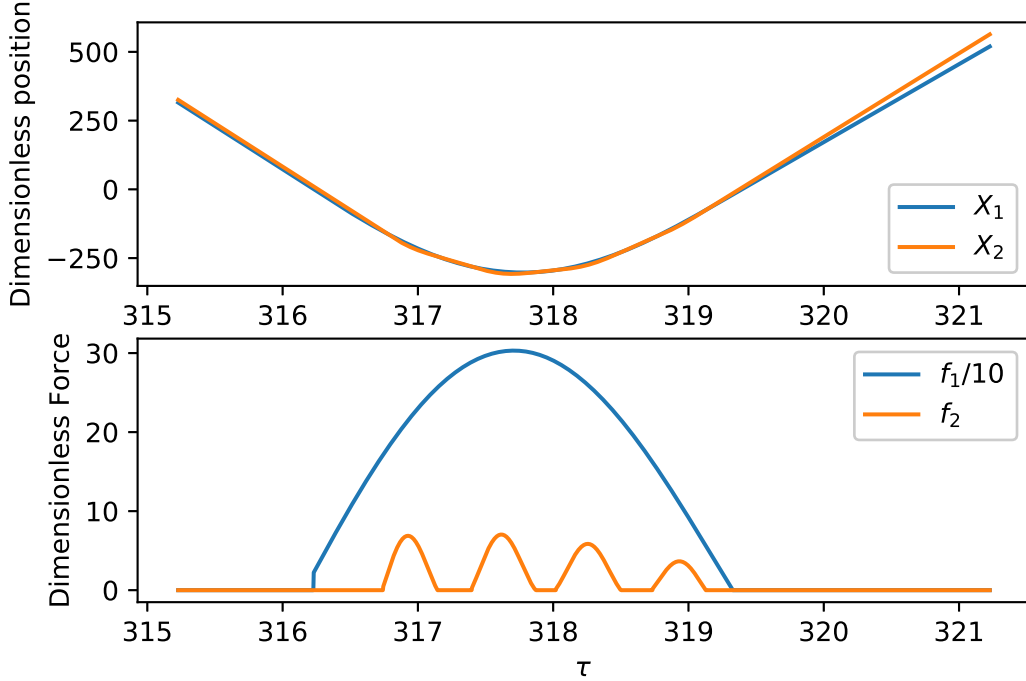


Figure 3: The trajectories of the balls and the force curves during the first collision are shown for a representative case where $\tau_d/\tau_f = 0.010$. In this case, $\mu = 0.010$, and $\varepsilon_1 = \varepsilon_2 = 0.9$.

mutual compression. The damping ratios are related to the coefficients of restitution [11] via

$$\varepsilon_1 = \exp \left[-\frac{\zeta_1}{\sqrt{\zeta_1^2 - 1}} \ln \left(\frac{\zeta_1 + \sqrt{\zeta_1^2 - 1}}{\zeta_1 - \sqrt{\zeta_1^2 - 1}} \right) \right] \quad (16)$$

$$\varepsilon_2 = \exp \left[-\frac{\zeta_2}{\sqrt{\zeta_2^2 - \frac{\mu}{1+\mu}}} \ln \left(\frac{\zeta_2 + \sqrt{\zeta_2^2 - \frac{\mu}{1+\mu}}}{\zeta_2 - \sqrt{\zeta_2^2 - \frac{\mu}{1+\mu}}} \right) \right], \quad (17)$$

with the principal branch cut used for the natural logarithm when the argument becomes complex. The expressions can be made manifestly real-valued in a piecewise fashion, as shown in Appendix A. The problem is now defined in terms of the three dimensionless constants μ , ε_1 , ε_2 , and two initial conditions $X_1(0)$, $X_2(0)$.

3.1 Condition for independent collisions

The duration of contact between the lower ball and the floor is calculated in the adiabatic approximation wherein the force from the upper ball has negligible effect [11]. The resulting

expression in dimensionless units is

$$\tau_f = \begin{cases} \frac{1}{\sqrt{1-\zeta_1^2}} \left(\pi - \arctan \frac{2\zeta_1\sqrt{1-\zeta_1^2}}{1-2\zeta_1^2} \right) & \text{for } \zeta_1 < \frac{1}{\sqrt{2}} \\ -\frac{1}{\sqrt{1-\zeta_1^2}} \arctan \frac{2\zeta_1\sqrt{1-\zeta_1^2}}{1-2\zeta_1^2} & \text{for } \frac{1}{\sqrt{2}} < \zeta_1 < 1 \\ -\frac{1}{\sqrt{\zeta_1^2-1}} \operatorname{artanh} \frac{2\zeta_1\sqrt{\zeta_1^2-1}}{1-2\zeta_1^2} & \text{for } \zeta_1 > 1. \end{cases} \quad (18)$$

This expression is exact in the case of independent collisions, or in the limit $\mu \rightarrow 0$. In other situations, the actual floor contact time will be longer. The value of τ_f is used to determine if the collisions are independent. The time interval between the time $X_1 = 0$ and $X_2 = 0$

$$\tau_d = \sqrt{2} \left(\sqrt{X_2(0)} - \sqrt{X_1(0)} \right). \quad (19)$$

This is interpreted as the time at which the balls would collide if they did not compress or bounce. If $\tau_d > \tau_f$, then the collisions are independent. Otherwise, the lower ball will still be in contact with the floor when the upper ball collides with it.

Figure 3 shows the trajectories of the two balls and the force curves during the lower ball's first collision with the floor. In this case, $\tau_d/\tau_f = 0.01$, but the first contact of the balls occurs later than 0.01 of the way between initial and final contact of the lower ball with the floor, due to the compression of the lower ball. (See Appendix B for details of the trajectories during this phase of motion.) The compression of the balls is illustrated by the fact that both X_1 and X_2 become negative in Figure 3.

For given values of ε_1 , ε_2 , and μ , the bounce height ratios are found to be the same if τ_d/τ_f is kept fixed. For different drop heights, the timing of the collision and the overall scale of the forces will change, but the overall form remains the same when τ_d/τ_f is held constant. Thus, the situation is described entirely by three parameters (ε_1 , ε_2 , μ) and a single initial condition (τ_d/τ_f).

4 Results from the linear dashpot model

Most analysis of the two-ball drop problem focuses on the first bounce [12], taken here to encompass the time from which the balls are released until the upper ball reaches its next local maximum in height. The collisions of interest for the first bounce include the first collision between the lower ball and the floor, and one or several collisions between the two balls. We extend our analysis to include the second bounce of the upper ball. The lower ball will contact the floor one or more times before the balls collide for the second time, and the second collision may or may not occur with the lower ball in contact with the floor.

To simplify the analysis, we set $\varepsilon_1 = \varepsilon_2$ throughout the rest of this work. In general, these coefficients of restitution may differ, but the results are shown to be qualitatively similar when $\zeta_1 = \zeta_2$ instead [9]. The ball parameters ε , μ and the initial condition τ_d/τ_f were each divided into 50 increments, for 50^3 parameter combinations. The ranges were taken as $\varepsilon \in (0.5, 1)$, $\mu \in (10^{-2}, 1)$ and $\tau_d/\tau_f \in (10^{-4}, 1)$. For the sake of comparison, the plots shown here focus primarily on the representative value of $\varepsilon = 0.816$, but animated

visualizations of all data are available [13]. We use a standard numerical ordinary differential equation solver[14, 15] to integrate the initial value problem (13, 14) with the balls released from rest.

4.1 Details of first bounce collisions

Analysis of the forces (15) from simulations with simultaneous contacts reveals multiple contacts between the two balls under a variety of conditions, consistent with the analysis in [9]. Figure 3 shows a case with four contacts between the balls, occurring entirely while the lower ball is in contact with the floor. Figure 4 shows a case where a second contact occurs just after the lower ball has left the floor.

The number of contacts between the two balls depends sensitively upon the ball parameters and initial condition. The count varies between one and twelve for the representative data shown in Figure 5, with $\varepsilon = 0.816$. Multiple contacts are mostly found when μ and τ_d/τ_f are small, so the plot axes are scaled logarithmically to show this detail, and the range of τ_d/τ_f is expanded to $(10^{-4}, 1)$.

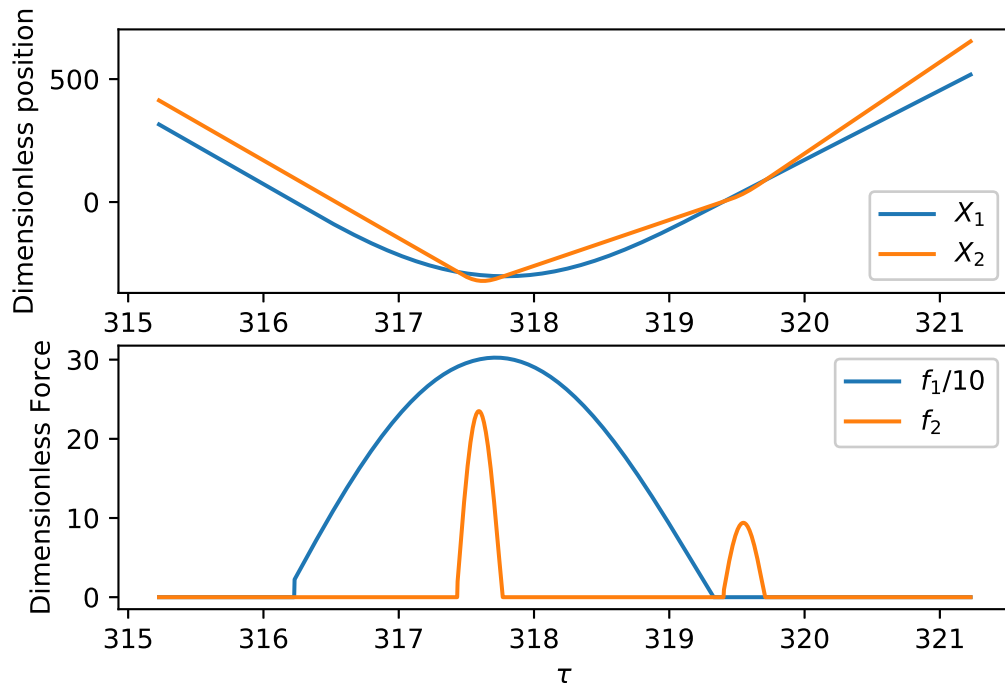


Figure 4: In this simulation, $\mu = 0.01$, $\tau_d/\tau_f = 0.1$, and $\varepsilon_1 = \varepsilon_2 = 0.9$. One of the collisions between the balls occurs just after the lower ball leaves the floor.

Because contact between the two balls is defined by $f_2 \neq 0$, instead of by the balls' positions, experimental setups that measure position only will not confirm or refute the details of the collisions presented here [16]. Piezoelectric sensors placed between the balls and on the floor present a more promising experimental setup, but the situations studied in [17] do not show clear evidence for multiple contacts. However, the particular measurements in that paper do not conflict with our simulations, as they do not match conditions predicted

to exhibit multiple collisions. Future experiments targeting the parameters that predict multiple contacts would help validate the use of this model.

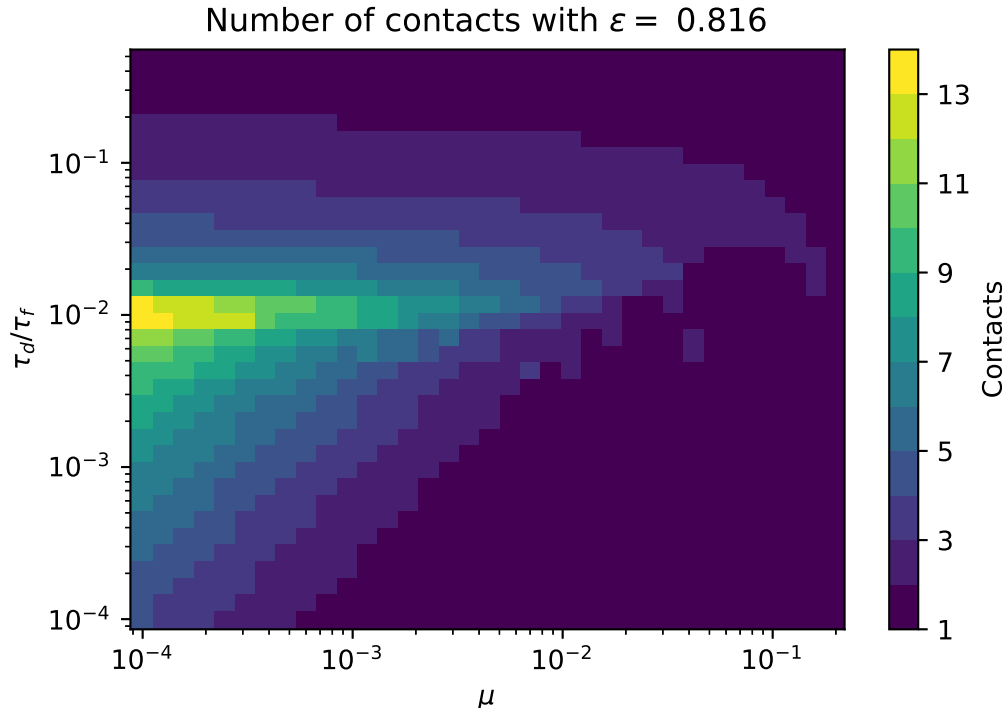


Figure 5: The number of contacts between the two balls during the first bounce with a typical coefficient of restitution $\varepsilon = 0.816$, chosen to be the same for both balls. The axes are logarithmically scaled to illustrate the effects found with small initial gaps and mass ratios.

4.2 Comparison of first bounce heights to ICM

While the details of the forces during the collision are interesting, the post-collision motion of the balls is more readily observable in an experimental setting. The analysis presented here focuses on the motion of the upper ball in part because the lower ball’s motion is largely unaffected by the collision for small mass ratios. We focus on the maximum height of this ball after each bounce rather than the relative velocity of the balls because the height of the second bounce is influenced by the post-collision velocity and the height of the second collision.

When the initial gap between the balls is small ($\tau_d/\tau_f \ll 1$), the height of the first bounce is less than the ICM prediction (4). The ICM limit is recovered in the case $\tau_d/\tau_f > 1$, as expected when collisions are independent. (Note that $\tau_d/\tau_f \gg 1$ results in collisions high above the floor. In this case the post-collision velocities will match the ICM, but the heights will not due to the height of the collision. These situations are not explored here.)

Intermediate gaps show more detailed structure. For some combinations of parameters, the bounce height remains below the ICM prediction, while for others the simulated bounce

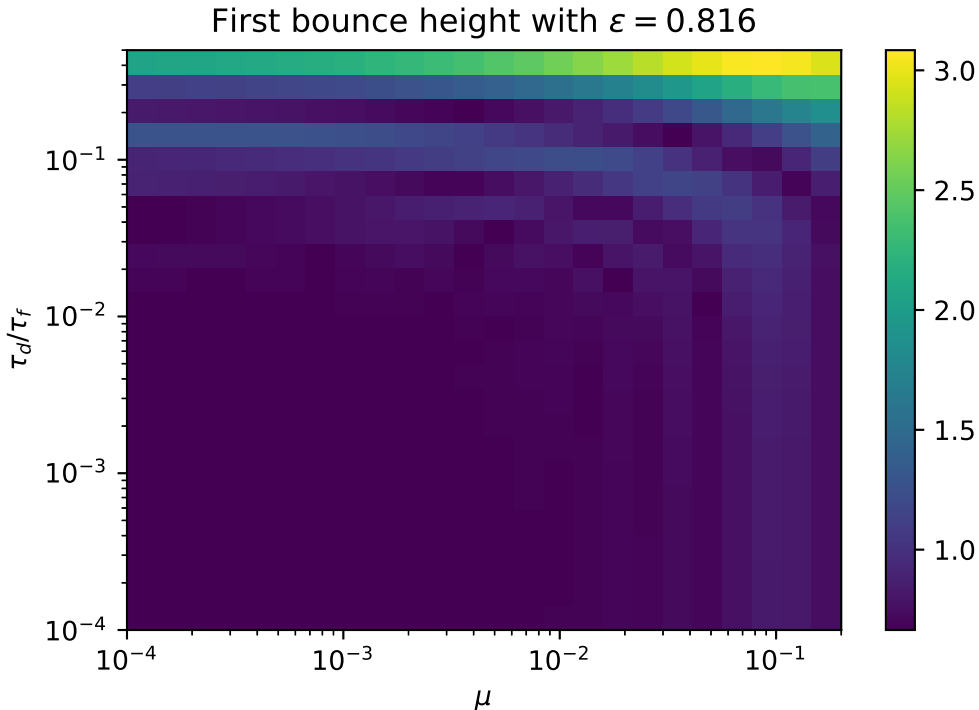


Figure 6: Comparison to Figure 5 shows no clear relationship between number of contacts and the height the upper ball reaches on its first bounce.

height is greater than that of the ICM. The ICM is overperformed when ε is small and μ is on the large end of the range studied, as shown in Figure 7. These conditions lead to small bounce heights, below the initial drop height, in any case.

The ICM closely approximates post-collision behavior for a variety of cases where the collisions are not truly independent, as $\tau_d/\tau_f < 1$. For $\tau_d/\tau_f \approx 0.7$, there is deviation from the ICM for some regions of the parameter space shown in Figure 8, but most situations are well-approximated by the simple model. Plots of larger values of τ_d/τ_f are not shown because they do not exhibit noticeable contrast, as all results are quite close to the ICM value. For example, the bounce heights are all within 5% of the ICM limit for $\tau_d/\tau_f > 0.85$ for the range of ball parameters studied. This unexpected success of the ICM is confirmed by experimental measurements [16, 17].

4.3 Second bounce

In this section, we analyze the height of the upper ball on the second bounce, specifically studying the delayed rebound effect with the second bounce higher than the first. Figure 9 shows a comparison of the second bounce height to the height of the first bounce using $\varepsilon = 0.816$ as an illustrative example. This plot shows that most cases of the delayed rebound effect occur for small initial drop gaps and small mass ratios, Qualitatively resembling the ICM result in Figure 2. The region expands as ε increases. As expected, the small mass-ratio limits are approximately achieved in the elastic case ($\varepsilon = 1$), when the initial collisions

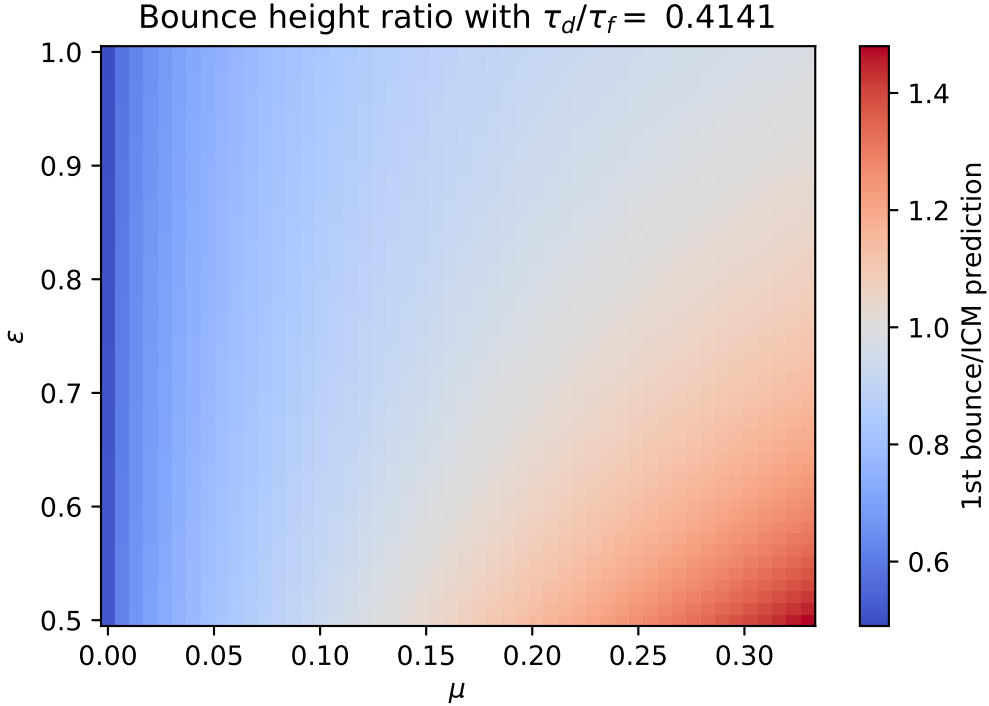


Figure 7: For moderate initial gaps, as shown here, there are some combinations of ϵ , μ that result in bounces lower than the ICM prediction, while others result in bounces higher than the ICM. The ratios plotted range from 0.49 to 1.48.

between the floor and the two balls are independent ($\tau_d/\tau_f = 1$).

In Figure 10, the first and second bounce heights are compared. It is evident that the delayed rebound effect is most prominent in cases where the first bounce is low, often lower than the initial drop height. The highest second bounces on an absolute scale occur when the first bounce is also high. Some of these do slightly exceed the first bounce, but these cases are relatively few.

Visual inspection gives a general sense of the causes of the delayed rebound effect that is confirmed by systematic comparison. For the parameter ranges studied, 12.3% of combinations resulted in the delayed rebound effect. Of these, 93% occurred in cases where the first bounce was lower than the ICM prediction. However, having a first bounce lower than the ICM prediction was not highly predictive; only 22% of these cases have a higher second bounce.

Typically, the lower ball is not in contact with the floor when the balls collide for the second bounce, and the balls make a single contact with each other. When the lower ball is in contact with the floor, multiple contacts between the balls are possible, in a manner that is qualitatively similar to the first bounce. These cases lead to a noticeably lower second bounce than others in nearby parameter space.

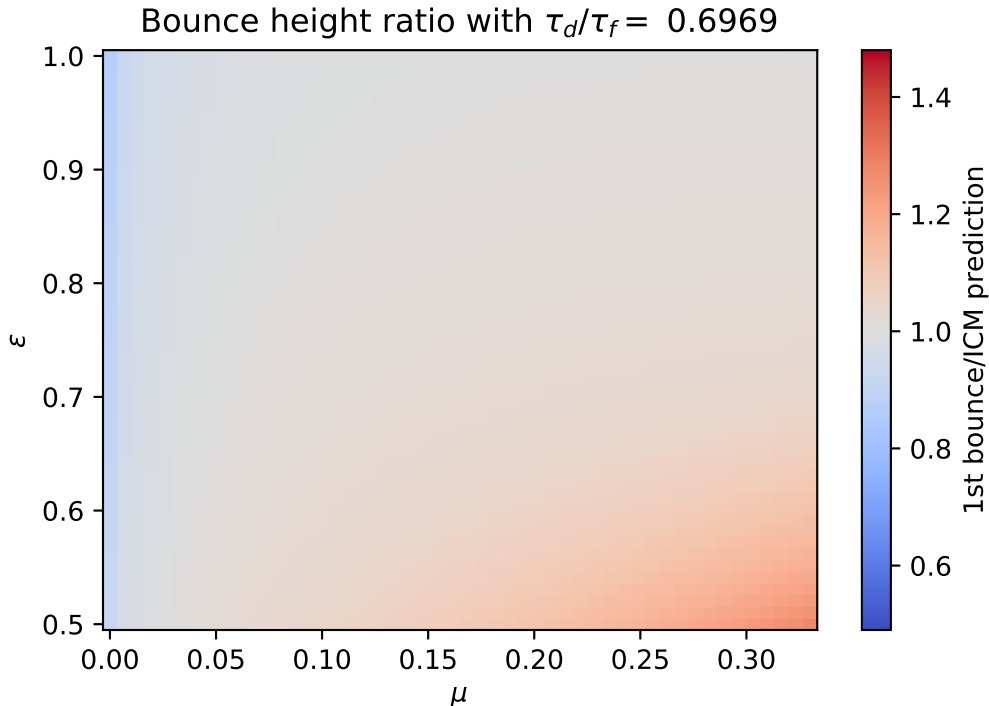


Figure 8: The results of the simulation begin to converge to the ICM result for a wide range of ϵ , μ , despite the collisions not being independent, with $\tau_d/\tau_f < 1$. The ratios plotted range from 0.87 to 1.27.

5 Conclusions

We show that the “delayed rebound effect,” where the second bounce of two aligned balls is higher than the first, is present in both a semi-analytic independent contact model (ICM) and the numerical solutions to a linear dashpot force between the balls. The effect is most prominent when the upper ball has a much smaller mass than the lower ball, and the distance gap between the balls is small when they are released. Typically, the finite duration of the collisions leads the first bounce to be smaller than predicted by the ICM, so the expected high bounce does not come until the second bounce. This is consistent with the informal observation that inspired this study: namely, that the delayed rebound effect is more commonly seen in ping-pong ball–basketball collisions than in tennis ball–basketball collisions.

Rather than focus on the parameters of a few particular sports balls, we look for universal behavior. The relevant ball parameters are reduced to the mass ratio $\mu = m_1/m_2$ and the coefficient of restitution ϵ , assumed to be the same for both balls. The initial conditions of drop height and gap between the balls is reduced to a single parameter τ_d/τ_f , which characterizes the time between the lower ball reaching the floor and the two balls making first contact. This approach represents a simplification over previous studies, and can be generalized to more than two balls.

We examined the details of the first bounce collisions, finding multiple contacts be-

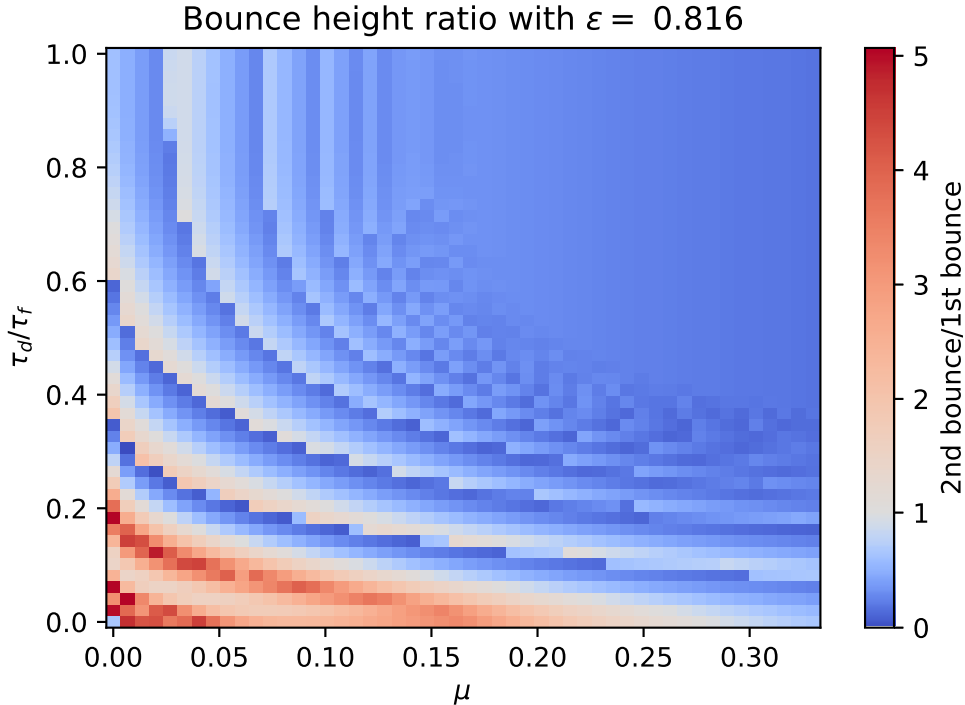


Figure 9: Comparison of the second bounce height to the first bounce height. Red points indicate situations in which the second bounce is higher than the first.

tween the balls in some cases. However, the multiple impacts did not correlate with the post-collision dynamics of the balls. For the first bounce, we found that small initial gaps resulted in bounces that were smaller than the ICM prediction, while the ICM is approximately correct for larger initial gaps, despite the overlapping collisions. This corresponds to experimental and theoretical results, albeit with a greatly simplified description of the contact force than in [16]. Direct comparison to realistic ball parameters for both first and second bounces is reserved for future work.

While [9] suggests that the linear dashpot model gives qualitatively similar results to simulations using the Hertz force, [18] finds qualitatively different results between these forces when studying chain collisions. Thus, it may be worthwhile to repeat this study with a Hertzian contact force, more appropriate for viscoelastic spheres.

A thorough experimental study of the delayed rebound effect requires a mechanism to constrain the interacting particles to a single dimension. Precisely aligned spheres, as used in experimental studies of the first bounce, are unlikely to remain aligned for a second bounce. Low friction carts on an inclined track, with springs for repulsion, may be a useful model, although it might be difficult to achieve the range of mass ratios seen in ball drop experiments.

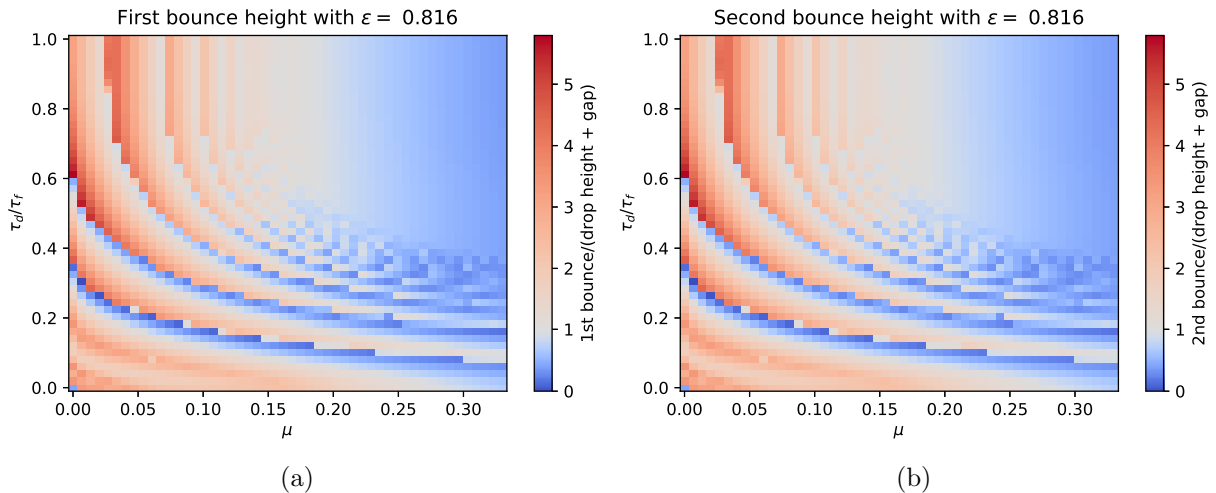


Figure 10: Comparison of bounce heights to the initial height for a representative value of the coefficient of restitution. The plot in (a) shows that the first bounce exceeds the drop height in most regions of parameter space. In (b), we see more detailed structure for the second bounce.

Acknowledgments

Thanks to Joe West for suggesting that my observation of my apparently failed classroom demo could be turned into a paper. Numerical simulations were performed using NumPy and SciPy. The second bounce of the ICM was analyzed using Mathematica.

The two-ball drop problem was the first physics problem that ever fascinated me, beginning with a demo at an IUPUI Saturday science program for high school students. Thanks to the Macalester students who didn't hold it against me when my overly-enthusiastic rendition of this demo resulted in a broken light bulb falling precariously close to them. Thank you to the Indiana State students for their patience as I repeated the seemingly unremarkable ping-pong version of the demo. Maybe the reason for my fascination is now evident.

I want to show my appreciation to my dog, Luna, who faithfully sat at my feet during the researching and writing of this paper during the COVID-19 quarantine. Good girl.

A Explicitly real coefficients of restitution

The expressions for the coefficients of restitution in (16,17) are both real-valued, but require the handling of the natural logarithm of complex numbers. The following piecewise

expressions are explicitly real-valued, and match the expressions in the main text.

$$\varepsilon_1 = \begin{cases} \exp \left[-\frac{\zeta_1}{\sqrt{1-\zeta_1^2}} \left(\pi - \arctan \frac{2\zeta_1\sqrt{1-\zeta_1^2}}{1-2\zeta_1^2} \right) \right] & \text{for } \zeta_1 < \frac{1}{\sqrt{2}} \\ \exp \left[\frac{\zeta_1}{\sqrt{1-\zeta_1^2}} \arctan \frac{2\zeta_1\sqrt{1-\zeta_1^2}}{1-2\zeta_1^2} \right] & \text{for } \frac{1}{\sqrt{2}} < \zeta_1 < 1 \\ \exp \left[-\frac{\zeta_1}{\sqrt{\zeta_1^2-1}} \ln \left(\frac{\zeta_1+\sqrt{\zeta_1^2-1}}{\zeta_1-\sqrt{\zeta_1^2-1}} \right) \right] & \text{for } \zeta_1 > 1. \end{cases} \quad (20)$$

$$\varepsilon_2 = \begin{cases} \exp \left[-\frac{\zeta_2}{\sqrt{\frac{\mu}{1+\mu}-\zeta_2^2}} \left(\pi - \arctan \frac{2\zeta_2\sqrt{(1+\mu)(\mu-\zeta_2^2(1+\mu))}}{\mu-2\zeta_2^2(1+\mu)} \right) \right] & \text{for } \zeta_2 < \sqrt{\frac{\mu}{2(1+\mu)}} \\ \exp \left[\frac{\zeta_2}{\sqrt{\frac{\mu}{1+\mu}-\zeta_2^2}} \arctan \frac{2\zeta_2\sqrt{(1+\mu)(\mu-\zeta_2^2(1+\mu))}}{\mu-2\zeta_2^2(1+\mu)} \right] & \text{for } \sqrt{\frac{\mu}{2(1+\mu)}} < \zeta_2 < \sqrt{\frac{\mu}{1+\mu}} \\ \exp \left[-\frac{\zeta_2}{\sqrt{\zeta_2^2-\frac{\mu}{1+\mu}}} \ln \left(\frac{\zeta_2+\sqrt{\zeta_2^2-\frac{\mu}{1+\mu}}}{\zeta_2-\sqrt{\zeta_2^2-\frac{\mu}{1+\mu}}} \right) \right] & \text{for } \zeta_2 > \sqrt{\frac{\mu}{1+\mu}}. \end{cases} \quad (21)$$

B Trajectory of lower ball in contact with the floor

While the lower ball is in contact with the floor, its position is the trajectory of a damped harmonic oscillator

$$X_1(\tau) = \frac{1}{\cos p} \cos \left(\tau \sqrt{1-\zeta_1^2} + p \right) e^{-\zeta_1\tau} - 1, \quad (22)$$

where $\tau = 0$ is redefined as the time at which the lower ball first contacts the floor, and

$$p = \arctan \frac{\zeta_1 + \sqrt{2H}}{\sqrt{1-\zeta_1^2}}. \quad (23)$$

Here, $H = h/x_c$ is the dimensionless drop height.

During this motion, the upper ball is in free fall. When the lower ball hits the ground, the position of the lower ball is $X_2(0) = \Delta H$, the initial gap in dimensionless coordinates. The time-dependent position is

$$X_2(\tau) = \Delta H - \sqrt{2H}\tau - \tau^2. \quad (24)$$

Solving for the time and position of collision requires solving a transcendental equation, assuming $\tau_d < \tau_f$, as discussed in Section 3.1. Because of this, there is little practical reason to prefer this method over the computational simulations performed. In either case, it is shown that the actual time to collision is greater than τ_d . Equation (22) assumes an adiabatic approximation, where the path of the lower ball is unaffected by collision(s) with the upper ball. The expression becomes exact in the limit $\mu \rightarrow 0$ or in the case $\tau_d > \tau_f$.

References

- [1] W. R. Mellen, “Superball Rebound Projectiles,” *American Journal of Physics* **36** no. 9, (Sept., 1968) 845–845.
- [2] W. G. Harter, “Velocity Amplification in Collision Experiments Involving Superballs,” *American Journal of Physics* **39** no. 6, (June, 1971) 656–663.
- [3] F. Herrmann and P. Schmlzle, “Simple explanation of a well-known collision experiment,” *American Journal of Physics* **49** no. 8, (Aug., 1981) 761–764.
- [4] J. D. Kerwin, “Velocity, Momentum, and Energy Transmissions in Chain Collisions,” *American Journal of Physics* **40** no. 8, (Aug., 1972) 1152–1158.
- [5] P. Patrício, “The Hertz contact in chain elastic collisions,” *American Journal of Physics* **72** no. 12, (Nov., 2004) 1488–1491, [arXiv:0402036](https://arxiv.org/abs/0402036) [physics.ed-ph].
- [6] M. Kire, “Astroblaster—a fascinating game of multi-ball collisions,” *Physics Education* **44** no. 2, (Feb., 2009) 159–164.
- [7] M. Gharib, A. Celik, and Y. Hurmuzlu, “Shock Absorption Using Linear Particle Chains With Multiple Impacts,” *Journal of Applied Mechanics* **78** no. 3, (May, 2011) 031005.
- [8] B. Ricardo and P. Lee, “Maximizing kinetic energy transfer in one-dimensional many-body collisions,” *European Journal of Physics* **36** no. 2, (Feb., 2015) 025013.
- [9] Mller, Patric and T. Pschel, “Two-ball problem revisited: Limitations of event-driven modeling,” *Physical Review E* **83** no. 4, (Apr., 2011) 041304, [arXiv:1009.6153](https://arxiv.org/abs/1009.6153) [physics.class-ph].
- [10] D. Gugan, “Inelastic collision and the Hertz theory of impact,” *American Journal of Physics* **68** no. 10, (Sept., 2000) 920–924.
- [11] T. Schwager and T. Pschel, “Coefficient of restitution and lineardashpot model revisited,” *Granular Matter* **9** no. 6, (Nov., 2007) 465–469, [arXiv:0701278](https://arxiv.org/abs/0701278) [cond-mat.soft].
- [12] J.-H. Ee and J. Lee, “Magic mass ratios of complete energy-momentum transfer in one-dimensional elastic three-body collisions,” *American Journal of Physics* **83** no. 2, (Jan., 2015) 110–120, [arXiv:1310.5200](https://arxiv.org/abs/1310.5200) [physics.class-ph].
- [13] S. Bartz, “Data and visualizations.” <https://seanbartz.com/research/data-and-visualizations/>.
- [14] A. C. Hindmarsh, “ODEPACK, A Systematized Collection of ODE Solvers,” *IMACS Transactions on Scientific Computation* **1** (1983) 55–64.

- [15] L. R. Petzold, “Automatic selection of methods for solving stiff and nonstiff systems of ordinary differential equations,” *SIAM Journal on Scientific and Statistical Computing* **4** no. 1, (1983) 136–148.
- [16] Y. Berdeni, A. Champneys, and R. Szalai, “The two-ball bounce problem,” *Proc. R. Soc. Lond. A* **471** no. 2179, (July, 2015) 20150286.
- [17] R. Cross, “Vertical bounce of two vertically aligned balls,” *American Journal of Physics* **75** no. 11, (Oct., 2007) 1009–1016.
- [18] E. J. Hinch and S. Saint-Jean, “The fragmentation of a line of balls by an impact,” *Proc. R. Soc. Lond. A* **455** no. 1989, (Sept., 1999) 3201–3220.